Photochemical & Photobiological Sciences

Accepted Manuscript

This is an *Accepted Manuscript*, which has been through the Royal Society of Chemistry peer review process and has been accepted for publication.

Accepted Manuscripts are published online shortly after acceptance, before technical editing, formatting and proof reading. Using this free service, authors can make their results available to the community, in citable form, before we publish the edited article. We will replace this *Accepted Manuscript* with the edited and formatted *Advance Article* as soon as it is available.

You can find more information about *Accepted Manuscripts* in the Information for Authors.

Please note that technical editing may introduce minor changes to the text and/or graphics, which may alter content. The journal's standard Terms & Conditions and the Ethical guidelines still apply. In no event shall the Royal Society of Chemistry be held responsible for any errors or omissions in this *Accepted Manuscript* or any consequences arising from the use of any information it contains.

ROYAL SOCIETY OF CHEMISTRY

www.rsc.org/pps

Photochemical & Photobiological Sciences
CREATED USING THE RSC LaTeX PCCP ARTICLE TEMPLATE – SEE www.rsc.org/electronicfiles FOR DETAILS
ARTICLE TYPE www. rsc.org/xxxxxx | XXXXXXXX

OLEDs as prospective light sources for microstructured photoreactors

Dirk Ziegenbalg,*[a] Günter Kreisel,[b] Dieter Weiß [c] and Dana Kralisch[d]

Received February 18, 2014, Accepted Xth XXXXXXXXX 20XX
First published on the web Xth XXXXXXXXXX 200X
DOI: 10.1039/b000000x

In this work, the use of OLEDs as light sources to initiate photochemical reactions is published for the first time. A newly developed modular photoreactor system utilising microstructured reactors was equipped with commercially available OLED panels. The technical feature of being a surface emitter, the low thickness and the potentially high luminescent efficiency give reason to expect this kind of light source to be well suited for photochemical reactions. The reactor system was investigated by using photooxygenations as benchmark reactions. In detail photosensitised [4+2]-cycloadditions and [2+2]-cycloadditions of $^1O_2$ were examined beside Schenck-*ene*-reactions. It was demonstrated that OLEDs can successfully be used for conducting photochemical reactions. Moreover the equilibrium concentration of $^1O_2$ can be increased by varying the process conditions. Based on the experimental investigations, a reactor comparison showed that, with respect to productivity and efficiency data, the investigated microstructured photoreactors is currently not outperforming conventional batch reactors.

1 Introduction

Photochemical reactions are fundamental for live on earth. Interestingly the role of this reaction type in (industrial) chemistry is disparate less prominent. With view on the use of photoreactions in chemical laboratories Albini and Fagnoni [1] calculated that only 1 % of all published papers classified as organic syntheses by Chemical Abstracts involve a photochemical step.

Compared to thermal reactions, the number of photochemical processes on industrial scale is small. Examples are halogenations or sulfochlorinations which are large scale processes while other prominent production processes like the synthesis of vitamins or rose oxide are conducted on a far smaller scale. Photochemical processes are more frequently used for the production of intermediates and fine chemicals[2].

This finding may be attributed to the complex interplay of mass, heat, momentum and radiation transfer. Especially the radiation transfer should be highlighted at this point. The exponential character of the absorption results in a steep gradient of the photon flux. With this it becomes challenging to ensure a sufficient reaction control, especially when dealing with consecutive and/or parallel reactions[3,4].

This additional complexity is likely to be the reason why the value and potential of photochemical reactions are often under estimated. To conduct a cascade of e.g. two or three thermal reactions is often thought to be easier as conducting one photochemical reaction resulting the same product.

Since the reaction engineering part of photochemical reactions is challenging it is obvious to search for possibilities to tackle the problems. Beside other approaches this search might start with an evaluation of the reactor components.

While the most important decision for conducting photochemical reactions is the choice of the light source, the variety of artificial light sources is confined[5,6]. Beneath classical light sources such as mercury or sodium vapour and xenon arc lamps, light emitting diodes (LED) became popular during the last decade[2]. The prominent difference to classical light sources is a roughly monochromatic emission. This offers the possibility to choose a LED with a suited wavelength and relinquish filter. In sum this reduces energy losses caused by not usable photons. Further it is often claimed that LEDs offer a superior (luminescent) efficiency and that the small size offers new construction possibilities. In addition the magnitude of the photon flux is better suited for small scale laboratory needs. All this points resulted in various publications on this topic[7–12].

As a second important component a suitable photoreactor has to be chosen. The reactor choice is mainly driven by the need of providing a high photon flux within the reaction solution and a minimum of not irradiated volumes. Therefore common reactors are immersion or (falling) film reactors. Im-

[a] *Institut für Technische Chemie, Universität Stuttgart, Pfaffenwaldring 55, 70569 Stuttgart, Germany. Fax: +49 711 685 64065; Tel: +49 711 685 64285; E-mail: dirk.ziegenbalg@itc.uni-stuttgart.de*
[b] *Institut für Technische Chemie und Umweltchemie, Friedrich-Schiller-Universität Jena, Lessingstraße 12, 07743 Jena, Germany*
[c] *Institut für Organische Chemie und Makromolekulare Chemie, Friedrich-Schiller-Universität Jena, Humboldtstraße 10, 07743 Jena, Germany*
[d] *Institut für Pharmazie, LS für Pharmazeutische Technologie, Friedrich-Schiller-Universität Jena, Otto-Schott-Str. 41, 07745 Jena, Germany*

mersion reactors are mainly chosen because this kind of reactor fits best with the geometry of conventional light sources while (falling) film reactors are chosen when a thin fluid film or a high surface area of the liquid is needed[2,6].

LEDs are typically used for the irradiation of photomicroreactors. In early publications this combination was chosen to compensate the low photon flux by which LEDs were characterised at this time. Small reaction channels provide a low fluid thickness and therefore a better irradiation of the solution[7,8].

In this article the use of organic light emitting diodes (OLED) to initiate photochemical reactions will be demonstrated for the first time. The characteristics of this new kind of light source will be discussed and an adapted modular photoreactor will be shown. This will be followed by experimental investigations.

2 Organic Light Emitting Diodes

LEDs are well established as light sources to initiate photochemical reactions for some years now[9–12]. In almost all cases the published work focused on lab scale synthesis where the advantages of LEDs seem to be utilised best.

In recent years the development of light emitting diodes utilising organic semiconductors gained increasing attention[13]. OLED-displays as often seen in consumer electronic devices such as mobile phones, tablets or TVs are available for quite some time. But this kind of light emitting device is not well suited for conducting photochemical reactions. Reasons for this are on the one hand that the low photon flux is not suited to ensure fast reaction rates and on the other hand that light sources which can display pictures and movies are simply over-engineered for chemical purposes. With this a demand for better suited OLED devices arises.

Recently the first organic light emitting diodes for "sole" room lighting became commercially available. Compared to OLED-displays the advantages are a reduced thickness, a simpler construction and the reduced electronic complexity.

While the emission from LEDs is released from one small spot, OLEDs emit light from the complete area of the organic semiconductor. Since for photochemical reactions the projection area of a photoreactor has to be irradiated the general characteristics of OLEDs are better suited for irradiation of flat reactor devices. Furthermore it is possible to build flexible OLEDs which enables it to e.g. wrap the light source around a round reactor. This gives an additional degree of freedom for the construction of photoreactors since the light source can be adapted to the reactor geometry.

Within this work ORBEOS CDW-031 OLED panels from OSRAM Opto Semiconductors GmbH (Regensburg, Germany) were used[14]. This light source possesses a light output area with a diameter of 79 mm resulting in a light emitting

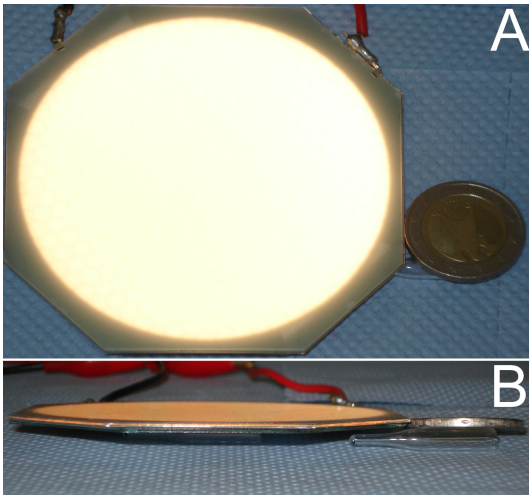

Fig. 1 A Top and **B** side view of one OLED panel.

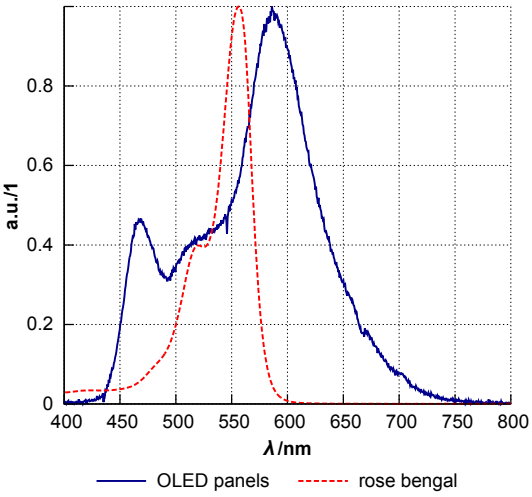

Fig. 2 Emission spectrum of the OLED panels and absorption spectrum of rose bengal.

area of 4902 mm^2. The overall building height amounts to only 2.1 mm. The OLED panels were operated with a potential of 3.3 V and a current of 200 mA. Hence one OLED panel consumes an electrical power of 0.7 W. An irradiance of 8.44 W/m^2 was measured which can be translated to a photon flux density of $4.18 \cdot 10^{-5}$ mol s^{-1} m^{-2} by taking the emission spectrum into account. Therewith one OLED emits a photon flux of $2.05 \cdot 10^{-7}$ mol s^{-1}.

The OLED panels emit a virtual white light. This emission is generated by three layers of organic semiconductors, each emitting light with a different wavelength. With respect to photochemical processes this characteristic offers optimisation potential since for future applications a single wavelength, adapted to a specific reaction, might be chosen. A top view as

well as a side view of an OLED panel is shown in figure 1. The emitted spectrum as well as the absorption spectrum of rose bengal are shown in figure 2.

The efficiency of electricity to photon conversion for the white OLEDs used in this work is around 7 %. This is larger than the efficiency of tungsten lamps ("light bulbs") but lower than the efficiency of white LEDs. To have a fair comparison fluorescent lamps should be considered, too. This type of light sources is available with (luminescent) efficiencies of up to 40 %[3]. While these technical data can not compete with for instance LEDs the authors want to emphasise that OLED technology is still in its infants. The OLEDs used were first presented to the public in November 2009. In March 2012 OSRAM presented the next generation of ORBEOS OLED panels. The very high pace of development can be illustrated by the increase in luminescent efficiency. While the typical power consumption per panel was kept constant at 0.7 W the luminance increased to 2000 cd/m^2 which corresponds to an increase in luminescent efficiency by a factor of two within around 2.5 years[15].

3 Modular Microstructured Photoreactor

It is widely accepted that microstructured photoreactors are a suitable tool for conducting photoreactions[16–18]. The exponential decay of the photon flux can be counteracted by using thin fluid layers which are an intrinsic characteristic of microstructured reactors[19–23]. This enables the experimentalist to work within the linear segment of the decay curve. With this the description of the radiation field is reduced to a linear relation which allows an easier mathematical handling[24,25]. Using thin fluid layers further ensures a high photon flux in the complete fluid. Unwanted side reactions can be suppressed since the irradiation times can be reduced and therewith competing reactions are less pronounced. For demanding reaction sequences the improved irradiation characteristics can be coupled to the enhanced heat and mass transfer characteristics of microstructured reactors. The small hold up improves the safety and the continuous operation results in a constant product quality as well as the possibility for an easy change of process conditions.

In context of this work the use of photomicroreactors was investigated whether this reactor type can beneficially compensate the lower light intensity of the OLEDs. To explore the potential of OLEDs to initiate photochemical reactions a novel modular microreactor system applying this light source was developed. The requirements for such a reactor system were the following:

- possibility for fast exchange of reactors and light sources,
- separation of fluidic parts and electric parts,
- reduced photon loss,
- compact construction,
- easy upgrading by additional modules.

The core concept of the developed reactor system was based on a rack system. Therefore the reactor modules were designed in such a manner that the glass reactor could be plugged in from the front side of the module while the OLEDs were plugged in from the back side. This strategy enabled the separation of the fluidic from the electric parts. The reactor was fixed by screwing 1/4-28 fittings through a connection bar. The fittings seize up with the reactor and on the one hand seal the fluidic connection and on the other hand stabilize the physical connection between the reactor and the connecting bar. The entry port as well as the exit are located on the upper side of the reactor (see the red and black fittings in figure 5). The OLEDs were fixed with splints above and below the glass reactor. This ensured that the distance between the OLEDs and the glass reactor was constant. Each reactor module could be equipped with one or two OLEDs. The inner part of the modules was shielded from external light by metal plates which could be inserted in appropriate notches. In addition this measure ensured that the photons emitted by the OLEDs stay within the reactor module due to reflection. As a consequence this enhances the amount of obtainable photons.

The overall building height of one module was only 4 cm. An easy extensibility was realised by tacks at all corners and fitting notches on the opposite side. With this it was possible to stack several modules with almost no effort. A picture of a setup with two stacks assembled from three modules each and the back view of an opened reactor stack is shown in figure 3.

4 Photooxygenations

Photooxygenations can be used to incorporate molecular dioxygen into organic compounds[26–28]. Such reactions are for example used to synthesise rose oxide, being an elemental substance in the perfume industry. A photosensitiser is used to generate singlet oxygen from dissolved triplet oxygen. In a consecutive reaction $^1O_2$ can react with an organic reactant giving peroxides or hydroperoxides.

The reaction engineering demands of photooxygenations are challenging because a large incident photon flux as well as a good mass transfer of gaseous oxygen into the liquid phase has to be ensured. Due to the high absorption coefficient of most sensitiser dyes complete absorption of light occurs within a short distance even with low sensitiser concentration.

Both demands, a large photon flux and a fast mass transfer, can be met by using photomicroreactors.[29] With this photooxygenations seem to be ideal test reactions to characterise the modular reactor system equipped with OLEDs.

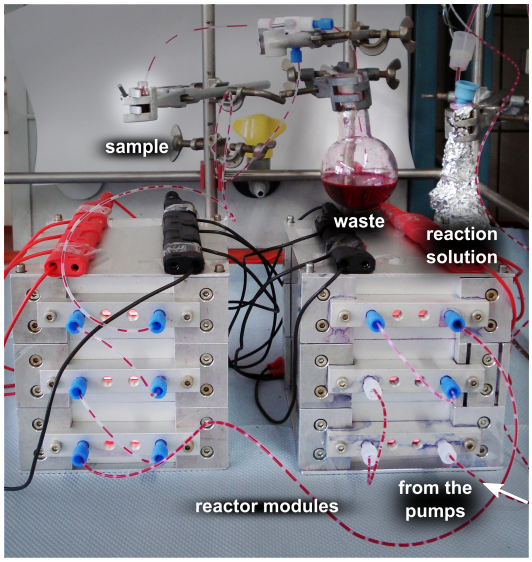

Fig. 3 A Reactor setup with two stacks assembled from three modules each. The aluminium foils protecting the feeding tubes against ambient light have been removed for clarity. **B** Back view of an opened reactor stack with three modules equipped with one OLED per module. The OLED irradiates the reactor from above.

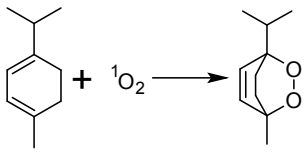

Scheme 1: Reaction scheme of the ascaridole synthesis.

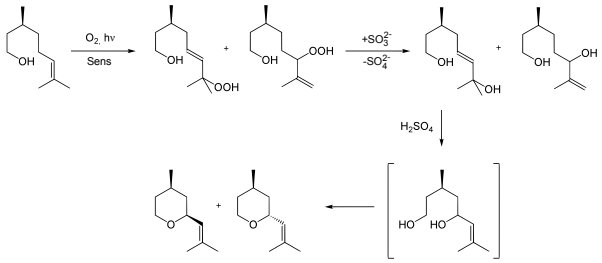

Scheme 2: Reaction scheme of the rose oxide synthesis.

As a first test reaction the synthesis of ascaridole from α-terpinene and $^1O_2$ was used (see scheme 1)[30]. α-terpinene reacts almost instantaneously via a [4+2]-cycloaddition with $^1O_2$. Under appropriate conditions this reaction might be used to assess the reactor. The amount of converted α-terpinene per unit of time can be correlated to the photon flux absorbed by the sensitiser per unit of time when the quantum yield for the $^1O_2$ generation of the sensitiser is known. Further the reaction rate of the [4+2]-cycloaddition should be at least 10, or better, 100 times higher then the rate of physical quenching.[31] Since the rate of physical quenching depends on the solvent, the used solvent should not be changed during assessment. The before mentioned requirements are fulfilled with the used reaction conditions. Hence this reaction is well suited to determine the utility of OLEDs and asses the reactor performance.

Furthermore alternative reaction pathways of photooxygenations were investigated. The before mentioned rose oxide can be synthesised starting from citronellol (see scheme 2)[6,8]. This reaction pathway first gives the corresponding hydroperoxides via a Schenck-*ene*-reaction. These compounds can be reduced to the alcohols in the next step. A last cyclisation step gives the desired rose oxide as a product. Since the focus of this work was on the photooxygenation step only the first reaction step was investigated.

Starting from naphthoquinone-derivatives, a number of biological active compounds are accessible[32,33]. For this class of substances 5-hydroxy-4-naphthoquinone (juglone) is a versatile building block for the synthesis of quinonoid compounds. Juglone can be obtained photosensitised from $^1O_2$ and 1,5-dihydroxynaphthalene (see scheme 3)[34,35]. Consequently this reaction was studied to further characterise the reactor system.

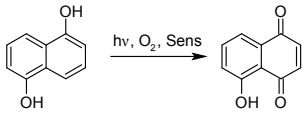

Scheme 3: Reaction scheme of the juglone synthesis.

1,2-dioxetanes are heterocyclic peroxides which can emit light when they decompose. This feature makes

1,2-dioxetanes suitable as luminescence marker in medical diagnostics[36,37]. Therefore the synthesis of dioxetanes via [2+2] photooxygenation was investigated by the reaction of 2-(3-methoxyphenyl)-3-methyl-1-benzofurane with $^1O_2$ (see scheme 4).

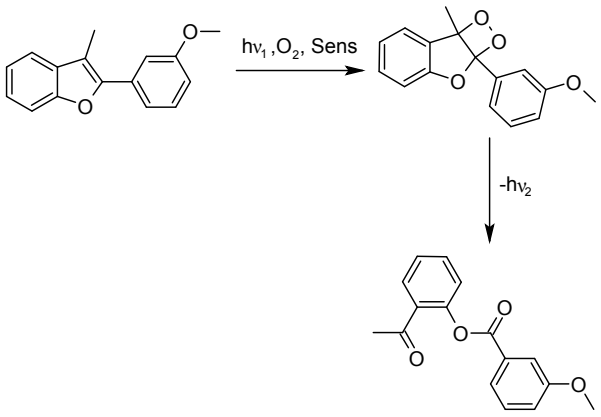

Scheme 4: Reaction scheme of the dioxetane synthesis.

5 Experimental section

The general flow chart of the reactor setup is shown in figure 4. The experiments were conducted with three serial connected reactor modules. The used reactors are made of borosilicate glass with round channels of 1 mm inner diameter and 1,6 m channel length per module (Little Things Factory GmbH, Ilmenau, Germany). With the 3 modules used in this work a total reactor volume of 3 × 1.256 mL = 3.768 mL was utilisable. Each reactor module was equipped with two OLEDs, one irradiating the reactor from above and one irradiating the reactor from below. Oxygen and the reaction solution were pumped with syringe pumps (neMESYS, cetoni GmbH, Korbußen, Germany). For each fluid two syringe pumps were coupled to realise continuous fluid delivery. The fluids were merged in a T-junction and depending on the process conditions a stable slug flow or an unstable slug flow resulted. The feeding tubes were shielded from ambient light by aluminium foils.

All reactions were conducted in methanol as solvent. All compounds were used as received without further purification. The starting concentrations of α-terpinene and citronellol were $\approx$ 0.14 mol L^{-1} while the concentration of 2-(3-methoxyphenyl)-3-methyl-1-benzofurane and 1,5-dihydroxynaphthalene were 0.12 mol L^{-1}. The reduced concentrations were caused by solubility limits. The purity of α-terpinene was declared to be $\geq$ 85 % but varied depending on the production lot. Therefore the purity of the reaction solution was determined by GC measurements before reaction and the actual concentration was used for further calcu-

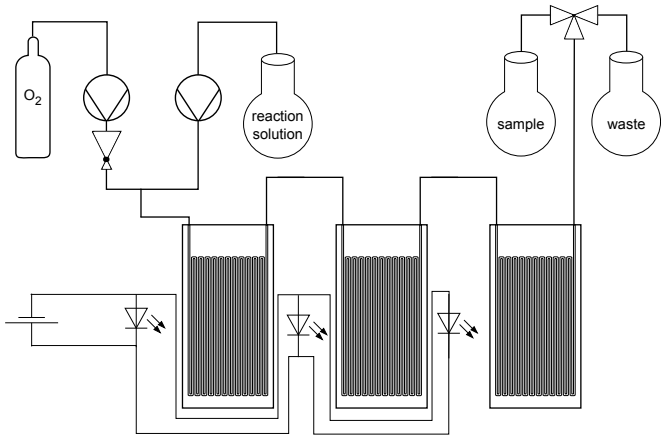

Fig. 4 General flow chart of the used reactor setup.

lations. Pure oxygen was used to provide $^3O_2$ to the liquid phase. As sensitiser rose bengal was used with an concentration of 0.0049 mol L^{-1}. This high concentration allowed the absorption of almost all photons reaching the reaction solution within the specific wavelength range. The absorption spectra of a diluted solution is shown in figure 2. Because of the small amount of substances, which were collected, the conversion of the reactants was monitored by GC measurements on a Varian CP-3900 apparatus equipped with a HP-5 column (30 m, 0.25 μm, d = 0.32 mm, 3 mL min^{-1} N_2; FID detector; injector temperature 175 °C, split injection mode, 1 μL; 35 °C maintained for 1 min, then ramped to 240 °C at 20 K min^{-1}). The spectral irradiance was measured by Carl Zeiss AG (Jena, Germany) with a CAS140CT-154 spectrometer (Instrument System, Munich, Germany) using a ISP250 integrating sphere (Instrument System, Munich, Germany).

The reactions were investigated with different process conditions. The total flow rate $\dot{V}$ of the two fluids and the stoichiometric input ratio of oxygen to reactant $r_{O_2/RL}$ were used as parameters. The stoichiometric input ratio is defined as the amount of oxygen entering the reactor per time divided by the amount of organic reactant entering the reactor per time. The flow rate mainly influences the residence time while the stoichiometric input ratio influences the flow conditions (stable or unstable slug flow) and the liquid's projection area. Figure 5 illustrates the different flow regimes. Using $r_{O_2/RL}$ = 0.5 a stable slug flow could be observed. Increasing $r_{O_2/RL}$ led to an unstable slug flow. The pressure which was build up due to friction of the liquid with the channel walls occasionally broke down. Thus liquid slugs were dissipated and the liquid was spread on the channel walls. This situation was stable for just a few seconds. After this the liquid accumulated and built up new slugs. In the following this behaviour repeated several times.

The conversions were fitted by statistical methods via a de-

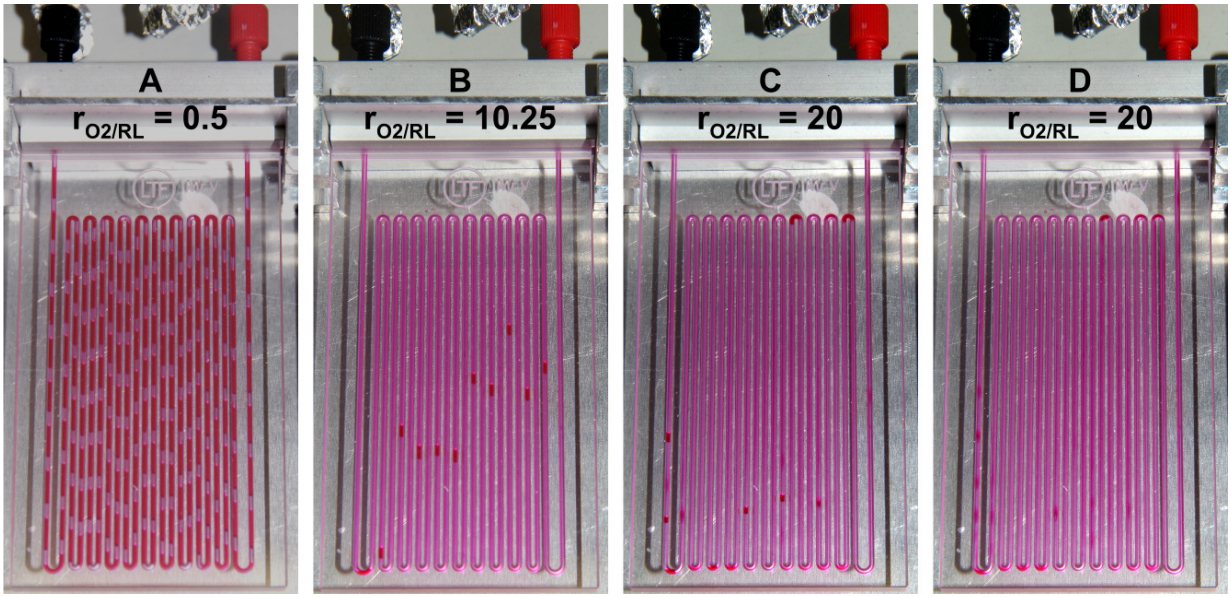

Fig. 5 Flow conditions observed during the experiments. **A** $r_{O_2/RL}$ = 0.5 – Stable slug flow. **B** $r_{O_2/RL}$ = 10.25 – Unstable slug flow, slugs break up after a certain travelling distance. **C** $r_{O_2/RL}$ = 20 – Unstable slug flow, slugs break up after a certain travelling distance. Picture was taken just before slug break up. **D** $r_{O_2/RL}$ = 20 – Unstable slug flow, slugs break up after a certain travelling distance. Picture was taken just after slug break up.

sign of experiment approach. In most cases the conversion was transformed into a logit representation to ensure that the fitting curve gives only values between 0 and 100 % conversion.

Additionally batch experiments were conducted to enable a comparison of the macroscopic reaction rate. If the same light sources are used this gives an impression on the efficiency of the photon input. Therefore a 250 mL round-bottom flask (14,3 cm inner diameter) was irradiated by three OLEDs. Oxygen was delivered through a PTFE-tube with a PTFE frit at the end. The frit was placed on the bottom of the round bottom flask. The oxygen flow rate was adjusted to around 20 mL min^{-1}. To prevent methanol from leaving the flask a reflux cooler was mounted on top of the round bottom flask. Preliminary experiments showed that the reaction rate could be improved by installing aluminium foils opposite the OLEDs. Consequently kinetic experiments were conducted with installed aluminium foils. The light sources and the aluminium foils where installed in direct contact to the glass to minimise photonic losses. To enable comparability to microreactor experiments additional experiments with three serial connected reactor modules were conducted while each module was equipped with one OLED irradiating the reactor from above.

6 Reaction kinetics

Photosensitised reactions are often described as zeroth order reactions. However, this is not entirely correct: Based on elemental steps a 2. order kinetic describes the reaction of e.g. $^1O_2$ and α-terpinene:

$$\frac{d[terpinene]}{dt} = k[^1O_2][terpinene]. \quad (1)$$

Usually this equation is reduced to a pseudo 1. order rate equation if the concentration of terpinene is much higher then the concentration of $^1O_2$. Since the $^1O_2$ is produced in a preceding sensitisation cycle the equilibrium concentration in steady state depends on the light intensity or, to keep the notations based on the amount of substance, the photon flux. This factor is typically neglected and "hidden" in the (overall) rate constant. This approach is allowed if the photon flux is stable over time which is the case for almost every laboratory lamp. With this assumptions the typically described zeroth order reaction kinetics of photochemical reactions should be properly called pseudo zeroth order reaction kinetics.

To continue with photooxygenations as an example this closer look on the reaction kinetics gives the explanation for typically used measures to increase the macroscopic reaction rate. A more powerful light source possesses a higher photon flux and with this a higher equilibrium concentration of $^1O_2$. Since this parameter limits the overall reaction rate the

use of a powerful light source speeds up photochemical reactions. This holds true only if the photochemical step is the rate limiting.

With this the apparent pseudo zeroth order rate constant should only be used for comparison if the setup is kept constant. Since the (apparent) reaction kinetics are the fundament of all productivity calculations a comparison of two photoreactor setups with both, different light sources and different reactors, results in a comparison of the incomparable. Therefore it is necessary to keep one of these parameters constant to ensure a comparable data bases.

If this boundary conditions are considered the reaction rate of a pseudo zeroth order reaction is equal to the space-time-yield (STY) defined as:

$$STY = \frac{n_R}{V_R \times \tau} = r_{0.\mathrm{Order}} = \left| -\frac{d[reactant]}{dt} \right| = k_{0.\mathrm{Order}}, \quad (2)$$

where n_R is the amount of converted reactant, V_R being the the inner reactor volume, t represents the irradiation/residence time and $k_{0.\mathrm{Order}}$ is the (apparent) rate constant of the reaction.

7 Results

7.1 Photooxygenations

The results for the synthesis of ascaridole are shown in figure 6. As expected a variation of the total flow rate results in a variation of the conversion. At $\dot{V}$ = 0.5 mL min^{-1} and $r_{O_2/RL}$ = 0.5 a conversion of 19 % could be measured, whereas 92 % conversion can be obtained with $\dot{V}$ = 0.5 mL min^{-1} and $r_{O_2/RL}$ = 20. Increasing the flow rate to $\dot{V}$ = 6 mL min^{-1} while keeping the stoichiometric input ratio constant reduces the conversion down to 3 % or 31 % for $r_{O_2/RL}$ = 0.5 and $r_{O_2/RL}$ = 20, respectively . This can be attributed to the reduced residence time. An increase of the stoichiometric input ratio while keeping the flow rate constant leads to an increase in conversion. There are two causes for this observation. First the amount of α-terpinene per unit time flowing through the residence time module is reduced. This naturally increases the conversion when the overall reaction rate stays the same, which is an intrinsic characteristic of pseudo zeroth order reactions. Second, the flow conditions change from a stable slug flow to an unstable slug flow. This reduces the thickness of the fluid films while increasing the projection area of the reaction solution. In combination this two effects result in an improved conversion.

Results for the first step of the synthesis of rose oxide are shown in figure 7. The trends are the same as for the synthesis of ascaridole but the conversion is in most cases a little bit lower. Since the reaction conditions are the same this indicates that the reaction rate of the *ene*-reaction is slightly

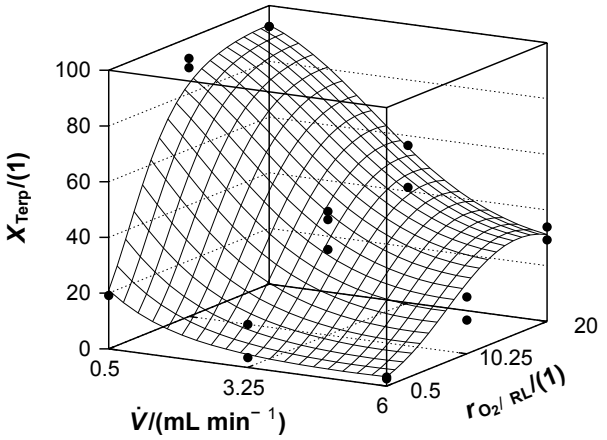

Fig. 6 Conversion of α-terpinene as a function of flow rate and stoichiometric input ratio.

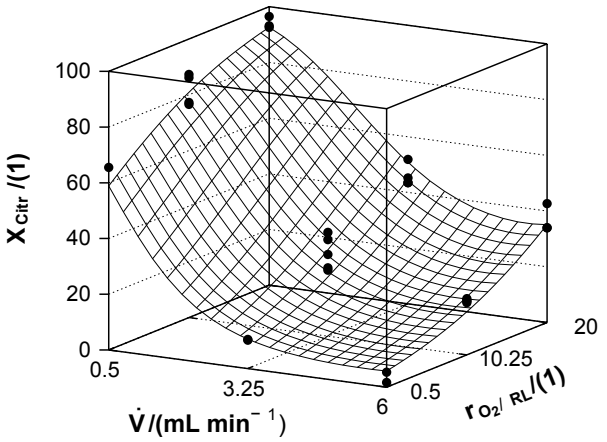

Fig. 7 Conversion of citronellol as a function of flow rate and stoichiometric input ratio.

slower then the rate of the [4+2]-cycloaddition. According to Wilkinson *et al.*[38] the rate constant of the cycloaddition is $k = 32 \cdot 10^6$ L mol^{-1} s^{-1} and for the *ene*-reaction is $k = 0.475 \cdot 10^6$ L mol^{-1} s^{-1}. This gives a difference of roughly 2 order of magnitude. Observing just slight differences in conversion for both reactions gives evidence to the assumption that the preceding $^1O_2$ generation is indeed rate limiting.

The results of the experiments with 1,5-dihydroxynaphthalene are shown in figure 8. Obviously the conversion is far lower then the conversions of α-terpinene or citronellol. The intrinsic rate constant of this reaction is $k = 1.8 \cdot 10^6$ L mol^{-1} s^{-1}.[38] While this rate constant lies between the rate constants of the cycloaddition and the Schenck-*ene*-reaction, the macroscopic rate constant is much lower. Since all reaction parameters and process conditions were kept the same, except the slightly lower starting concentration, it is surprising that such big

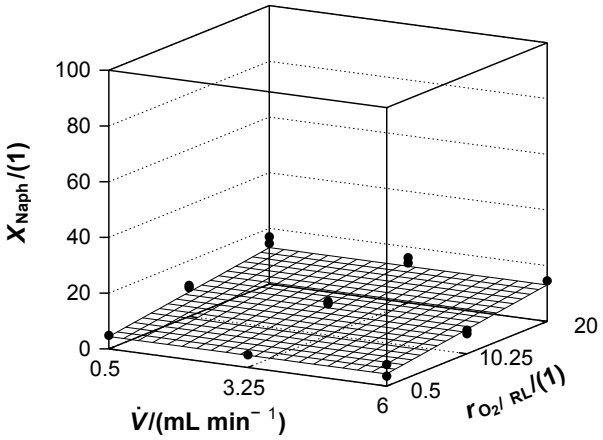

Fig. 8 Conversion of 1,5-dihydroxynaphthalene as a function of flow rate and stoichiometric input ratio.

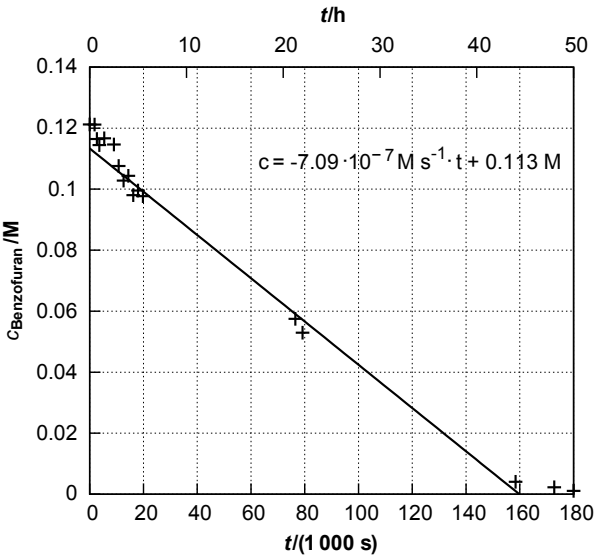

Fig. 9 Conversion of 2-(3-methoxyphenyl)-3-methyl-1-benzofurane as a function of reaction time.

differences occur. This can be attributed to the absorption of 1,5-dihydroxynaphthalene within the visible range. The reaction solution was coloured black by the reactant. This translates to a reduced photon flux at the sensitiser and with this to a decreased $^1O_2$ production. As a consequence the overall reaction rate is heavily reduced, too. This can be prevented by reducing the 1,5-dihydroxynaphthalene concentration or repeated sublimation of the reactant. Further the quantum yield of this reaction is lower than for the ascaridole synthesis or the reaction with citronellol leading to a decreased conversion when the same photon flux is available.[39]

First experiments with 2-(3-methoxyphenyl)-3-methyl-1-benzofurane resulted in very low conversion. Due to this it was decided to adapt the setup in such a manner that a recirculation of the reaction solution was possible. A total flow rate of $\dot{V}$ = 0.5 mL min^{-1} and a stoichiometric input ratio of $r_{O_2/RL}$ = 10.25 were chosen as process conditions. Taking samples at different times it was possible to estimate the macroscopic reaction rate. The results are shown in figure 9. Apparently the reaction follows a zeroth order macrokinetic. A rate constant of $k = 7.109 \cdot 10^{-7}$ L mol^{-1} s^{-1} could be calculated. After 44 h a conversion of 97 % could be obtained.

7.2 Reactor Evaluation

Gas-liquid reactions like photooxygenations may be limited by the mass transfer between the phases.[40–42] Investigations on the influence of the O_2 partial pressure revealed that the concentration of O_2 did not influence the mass transfer (not shown here). From this it can be concluded, that the reaction is not mass transfer limited under the investigated process conditions. More specific details will be given in a report with focus on a more detailed characterization of the reactor in terms of reaction engineering.

The temperature on the surface of the reactor modules was measured with Pt-100 temperature sensors during operation. The temperature stayed always below 35 °C. Hence a safe operation was ensured, even when synthesizing peroxides like ascaridole. An additional cooling was not necessary.

In figure 10 the results of the batch and corresponding flow experiments for the ascaridole synthesis are shown. Again a pseudo zeroth order correlation is observed. For the batch reactor a macroscopic rate constant of $k = 2.65 \cdot 10^{-7}$ L mol^{-1} s^{-1} can be calculated. The results for the microstructured photoreactor depend on the stoichiometric input ratio $r_{O_2/RL}$. For $r_{O_2/RL}$ = 0.5 a rate constant $k = 1.6 \cdot 10^{-5}$ L mol^{-1} s^{-1} can be calculated. Keeping in mind that the elemental kinetic is 2. order the difference can be attributed to an increase of the $^1O_2$ concentration by a factor of 100, when using the microstructured reactor. This can be further increased when the stoichiometric input ratio is changed to $r_{O_2/RL}$ = 10.25. A rate constant of $k = 8.9 \cdot 10^{-5}$ L mol^{-1} s^{-1} represents an increase in the $^1O_2$ concentration by a factor of 300 compared to the batch experiments. The differences between both flow experiments result from changing flow conditions. While with $r_{O_2/RL}$ = 0.5 a stable slug flow is observed, operating the reactor with $r_{O_2/RL}$ = 10.25 possesses an unstable slug flow. With this the fluid thickness is reduced significantly and in addition the projection area of the fluid is increased. This combination leads to an increase of the equilibrium concentration of $^1O_2$. Further increasing the stoichiometric input ratio has no additional effect on the reaction rate as can be concluded from the

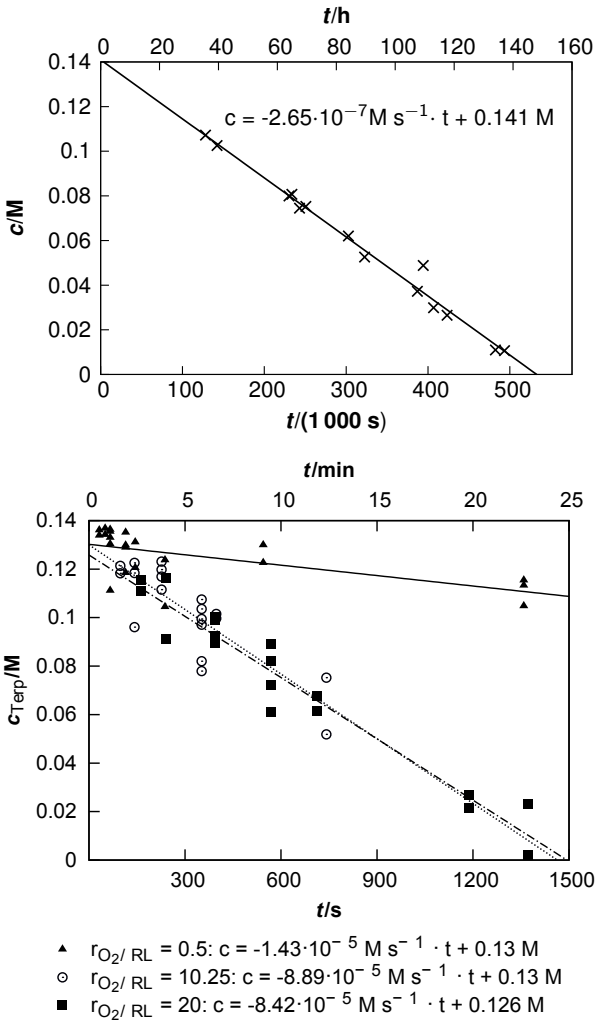

Fig. 10 Concentration as a function of time for the batch experiments (top) and for the continuous experiments (bottom).

results for $r_{O_2/RL} = 20$.

To get a good estimation of the investigated reactor setups the productivity $\dot{n}$ for the batch reactor and the microstructured photoreactor were calculated:

$$\dot{n} = \frac{n}{t}, \tag{3}$$

where n is the amount of converted α-terpinene and t is the reaction time. The productivity gives a more global view of the complete reactor setup. The results for the batch reactor and the microstructured photoreactor equipped with a different number of OLEDs are summarised in table 1. Only results with conversions higher then 95 % are shown and compared, since typically process conditions are chosen in such a manner that the effort of down stream cleaning processes is reduced. To ensure comparability between batch and flow experiments only the results for experiments with three OLEDs should compared directly. For this case the numbers demonstrate that the productivity $\dot{n}$ for the microstructured photoreactor (μPR) is similar to the productivity of the employed batch reactor.

A comparison between experiments using one OLED per module and experiments with two OLEDs per module shows that the productivity does not depend on the number of OLEDs per module but only on the stoichiometric input ratio.

These findings show that the expected advantages of microstructured photoreactors could not be verified in terms of productivity. This can be mainly attributed to an insufficient adaption of the used microstructured reactors to the emission characteristics of the light source. Due to the lag of taylor-made light sources the emission area of the OLEDs does not perfectly match the projection area of the residence time module (see e.g. figure 3). Beside this the advantages of continuous processing like constant product quality, easy handling and improved safety remain. From this it becomes clear, that to exploit the full potential of microstructured photoreactors the adaption of the reactors to the available light sources is a crucial task.

Levesque and Seeberger[43] presented a photochemical reactor possessing a high productivity. The authors also tested the reactor by conducting photooxygenations. The published results are also included in table 1 as the "FEP tube reactor". It becomes clear that the productivity of the FEP tube reactor is about 1 000 times higher then the values measured within this work. The crucial difference between the reactor presented by Levesque and Seeberger[43] and this work is the light source. Levesque and Seeberger[43] used a 450 W medium pressure mercury vapour lamp. This light source provides a much higher photon flux as the OLEDs used in this work. Hence a comparison based on the nominal energy consumption of the light source (neglecting further periphery) seems better suited. Therefore a specific productivity η_{el} is calculated:

$$\eta_{el} = \frac{\dot{n}}{P} = \frac{n}{E} \tag{4}$$

where $\dot{n}$ denotes the productivity and P is the nominal electrical power of the light source. This quantity represents the amount of substance generated per energy. The results show that it is possible to convert between 5 and 18 nmol reactant per Joule electrical energy with the μPR and OLEDs (see table 1). With the μPR the highest energy efficiency for the OLED photoreactor was observed when utilising one OLED per module, a stoichiometric input ratio of $r_{O_2/RL} = 10.25$ and a flow rate of $\dot{V} = 0.5$ mL min^{-1}. The results for the batch reactor are similar, while the literature reactor is 4.5 times more efficient. The better performance of the previously described reactor results mainly from the higher luminescent efficiency of the employed mercury lamp. While the electricity to light efficiency of such lamps is in the range between 30 and 40 %,

reactor	# of modules	light source	P/W	c/(mol/L)	$\dot{V}$/mL min^{-1}	$r_{O_2/RL}$/1	X/%	$\dot{n}$/(nmol/s)	η_{el}/(nmol/J)	ξ_R/(nmol/J)
μPR	3	3 OLEDs	2.1	0.14	0.5	10.25	94	37	18	252
μPR	3	3 OLEDs	2.1	0.14	0.5	20.0	95	20	10	136
μPR	3	6 OLEDs	4.2	0.14	0.5	10.25	98	39	10	133
μPR	3	6 OLEDs	4.2	0.14	0.5	20.0	98	20	5	68
batch	-	3 OLEDs	2.1	0.14	-	-	95	44	21	300
FEP tube[43]	-	med-p Hg	450	0.5	17	4	$\geq$95	41667	93	265

Table 1 Efficiency characteristics of the investigated μPR, the batch reactor and the FEP tube reactor in case of ascaridole synthesis[43].

the OLEDs are characterised by an efficiency of around 7 % (see above). To correct the specific productivity it can be divided by the electricity to light efficiency η:

$$\xi_R = \frac{\eta_{el}}{\eta} \quad (5)$$

The resulting values illustrate how efficient the photons, which are emitted by the light source, are used for the chemical reaction. Therefore this quantity will be called (energy based) photonic reactor efficiency ξ_R[44]. The results in table 1 show that the photonic reactor efficiency of the OLED photoreactor strongly depends on the number of OLEDs per module and the process conditions. To achieve a high photonic reactor efficiency of 252 nmol/J one OLED per module and as process conditions a flow rate of $\dot{V}$ = 0.5 mL min^{-1} and a stoichiometric input ratio of $r_{O_2/RL}$ = 10.25 should be used. Interestingly the batch setup shows an even higher photonic reactor efficiency of 300 nmol/J.

Assuming η = 35 % for the mercury vapour lamp, a photonic reactor efficiency of 265 nmol/J can be calculated for the literature reactor. Therefore both analysed flow reactors possess similar photonic efficiencies under optimised conditions. With this the reason for the differing productivities can be mainly attributed to a different photon flux of the light sources.

8 Conclusions

For the first time it could be shown that OLEDs are suitable light sources to initiate photochemical reactions. For this purpose commercially available OLED panels were used. To ensure an easy handling a modular photoreactor system utilising microstructured reactors was developed. This system was investigated with different kinds of photooxygenations. The results show that this type of reactions can be successfully conducted by using OLEDs. Furthermore it could be shown that the equilibrium concentration of $^1O_2$ can be increased by varying the process conditions.

As a consequence of the good technical properties of the light sources it seems possible that the use of OLEDs for visible light induced photoreactions becomes an alternative to already established light sources such as LEDs.

Based on the experimental investigations, a reactor comparison showed that, with respect on productivity and efficiency data, the investigated microstructured photoreactor does currently not outperform the conventional batch reactors.

Furthermore the gained results lead to the following conclusions for future developments of microstructured photoreactors: First, to further intensify photochemical reactions by using microstructured photoreactors, most effort should be invested in the optimisation of the photonic reactor efficiency. Second, to enable a comparison between literature data a standardised data base and evaluation procedure should be developed and used.

9 Acknowledgement

DZ thanks OSRAM Opto Semiconductors GmbH (Regensburg, Germany) for supplying OLED prototypes.

References

1 A. Albini and M. Fagnoni, *Nato. Sci. Peace. Secur.*, 2008, 173–189.
2 A. Griesbeck, M. Oelgemöller and F. Ghetti, *CRC Handbook of Organic Photochemistry and Photobiology*, CRC Press, 3rd edn, 2012.
3 H. Böttcher, *Technical Applications of Photochemistry*, Deutscher Verlag für Grundstoffindustrie, 1991.
4 C.-L. Ciana and C. G. Bochet, *Chimia*, 2007, **61**, 650–654.
5 M. A. Claria, H. A. Irazoqui and A. E. Cassano, *AIChE J.*, 1988, **34**, 366–382.
6 A. M. Braun, M.-T. Maurette and E. Oliveros, *Photochemical Technology*, John Wiley & Sons Ltd, 1991.
7 R. Gorges, S. Meyer and G. Kreisel, *J. Photoch. Photobio. A.*, 2004, **167**, 95–99.
8 S. Meyer, D. Tietze, S. Rau, B. Schäfer and G. Kreisel, *J. Photoch. Photobio. A.*, 2007, **186**, 248–253.
9 O. Shvydkiv, A. Yavorskyy, K. Nolan, A. Youssef, E. Riguet, N. Hoffmann and M. Oelgemöller, *Photochem. Photobio. S.*, 2010, **9**, 1601–1603.
10 O. Shvydkiv, A. Yavorskyy, S. B. Tan, K. Nolan, N. Hoffmann, A. Youssef and M. Oelgemöller, *Photochem. Photobio. S.*, 2011, **10**, 1399–1404.
11 J. M. Carney, R. J. Hammer, M. Hulce, C. M. Lomas and D. Miyashiro, *Tetrahedron Lett.*, 2011, **52**, 352–355.
12 J. Carney, R. Hammer, M. Hulce, C. Lomas and D. Miyashiro, *Synthesis*, 2012, **44**, 2560–2566.
13 T. Kalyani and S. Dhoble, *Renew. Sust. Energ. Rev.*, 2012, **16**, 2696–2723.

14 OSRAM Opto Semiconductors, *ORBEOS for OLED Lighting; CDW-031; Vorläufige Daten / Preliminary Data*, 2009.

15 OSRAM Opto Semiconductors, *ORBEOS for OLED Lighting; CDW-030; Engineering Sample Information - Status March 2012*, 2012.

16 H. Ehrich, D. Linke, K. Morgenschweis, M. Baerns and K. Jähnisch, *Chimia*, 2002, **56**, 647–653.

17 T. Fukuyama, Y. Hino, N. Kamata and I. Ryu, *Chem. Lett.*, 2004, **11**, 1430 – 1431.

18 Y. Matsushita, S. Kumada, K. Wakabayashi, K. Sakeda and T. Ichimura, *Chem. Lett.*, 2006, **35**, 410–411.

19 H. Lu, M. A. Schmidt and K. F. Jensen, *Lab Chip*, 2001, **1**, 22–28.

20 Y. Matsushita, T. Ichimura, N. Ohba, S. Kumada, K. Sakeda, T. Suzuki, H. Tanibata and T. Murata, *Pure Appl. Chem.*, 2007, **79**, 1959–1968.

21 E. E. Coyle and M. Oelgemöller, *Photochem. Photobio. S.*, 2008, **7**, 1313–1322.

22 M. Oelgemöller and O. Shvydkiv, *Molecules*, 2011, **16**, 7522–7550.

23 M. Oelgemöller, *Chem. Eng. Technol.*, 2012, **35**, 1144–1152.

24 A. E. Cassano, C. A. Martin, R. J. Brandi and O. M. Alfano, *Ind. Eng. Chem. Res.*, 1995, **34**, 2155–2201.

25 O. M. Alfano and A. E. Cassano, *International Journal of Chemical Reactor Engineering*, 2008, **6**, P2.

26 W. Rojahn and H.-U. Warnecke, *Dragoco-Report*, 1980, **27**, 159–164.

27 K. Gollnick, *Chim. Ind.*, 1982, **64**, 156–166.

28 M. C. DeRosa and R. J. Crutchley, *Coord. Chem. Rev.*, 2002, **233-234**, 351–371.

29 K. Jähnisch and U. Dingerdissen, *Chem. Eng. Technol.*, 2005, **28**, 426–427.

30 R. C. R. Wootton, R. Fortt and A. J. de Mello, *Org. Process. Res. Dev.*, 2002, **6**, 187–189.

31 J.-M. Aubry, B. Mandard-Cazin, M. Rougee and R. V. Bensasson, *J. Am. Chem. Soc.*, 1995, **117**, 9159–9164.

32 O. Suchard, R. Kane, B. J. Roe, E. Zimmermann, C. Jung, P. A. Waske, J. Mattay and M. Oelgemöller, *Tetrahedron*, 2006, **62**, 1467–1473.

33 O. Shvydkiv, C. Limburg, K. Nolan and M. Oelgemöller, *J. Flow Chem.*, 2012, **2**, 52–55.

34 M. De Min, M. Maurette, E. Oliveros, M. Hocquaux and B. Jacquet, *Tetrahedron*, 1986, **42**, 4953–4962.

35 M. De Min, S. Croux, C. Tournaire, M. Hocquaux, B. Jackquet, E. Oliveros and M.-T. Maurette, *Tetrahedron*, 1992, **48**, 1869–1882.

36 N. Wang and R. Hu, *Chemiluminescent Electron-Rich Aryl-Substituted 1,2-Dioxetanes*, Abbott Laboratories Technical Report WO9410258, 1994.

37 D. Heindl, H.-P. Josel, H. V. D. Eltz, H.-J. Hoeltke, R. Herrmann, R. Beckert, W. Adam and D. Weiss, *Heterocyclische Dioxetan-Substrate, Verfahren zur Herstellung und Verwendung*, Boehringer Mannheim Gmbh, 68305 Mannheim, Technical Report DE19538708A1, 1997.

38 F. Wilkinson, W. Helman and A. Ross, *J. Phys. Chem. Ref. Data*, 1995, **24**, 663–1021.

39 M. Oelgemöller, J. Mattay and H. Görner, *J. Phys. Chem. A*, 2011, **115**, 280–285.

40 R. A. Maurya, C. P. Park and D.-P. Kim, *Beilstein J. Org. Chem.*, 2011, **7**, 1158–1163.

41 C. P. Park, R. A. Maurya, J. H. Lee and D.-P. Kim, *Lab Chip*, 2011, **11**, 1941.

42 A. Yavorskyy, O. Shvydkiv, C. Limburg, K. Nolan, Y. M. C. Delaure and M. Oelgemöller, *Green Chem.*, 2012, **14**, 888–892.

43 F. Levesque and P. H. Seeberger, *Org. Lett.*, 2011, **13**, 5008–5011.

44 N. Serpone and A. V. Emeline, *Int. J. Photoenergy.*, 2002, **4**, 91–131.

The use of OLEDs to initiate photochemical reactions is demonstrated for the first time by conducting photooxygenations in a modular microstructured photoreactor.